Social network diversity and white matter microstructural integrity in humans

Tara Molesworth[1], Lei K. Sheu[2], Sheldon Cohen[1],
Peter J. Gianaros[2,3], Timothy D. Verstynen[1,3]

1) Department of Psychology, Carnegie Mellon University, Pittsburgh, PA
2) Department of Psychology, University of Pittsburgh, Pittsburgh, PA
3) Center for the Neural Basis of Cognition, Carnegie Mellon University and University of Pittsburgh, Pittsburgh, PA

Abbreviated Title:

Corresponding Author:
Timothy Verstynen, Ph.D.
Carnegie Mellon University
Department of Psychology & Center for the Neural Basis of Cognition
342C Baker Hall
Pittsburgh, PA 15213
timothyv@andrew.cmu.edu
412-268-4615 (phone), 412-624-9149 (fax)

Key Words: social network, diffusion tensor imaging, white matter, inflammation, connectivity, resting state fMRI

Figures: 5
Tables: 2
Words: 5,125

Conflict of Interest: The authors do not report any conflicts of interest.

Acknowledgements: This work was supported by National Institutes of Health grant HL089850, National Center for Complementary and Alternative Medicine award AT006694, and Pennsylvania Department of Health Formula Award #SAP4100062201.

Diverse aspects of physical, affective, and cognitive health relate to social integration, reflecting engagement in social activities and identification with diverse roles within a social network. However, the mechanisms by which social integration interacts with the brain are unclear. In healthy adults (N=155) we tested the links between social integration and measures of white matter microstructure using diffusion tensor imaging. Across the brain, there was a predominantly positive association between a measure of white matter integrity, fractional anisotropy (FA), and social network diversity. This association was particularly strong in a region near the anterior corpus callosum and driven by a negative association with the radial component of the diffusion signal. This callosal region contained projections between bilateral prefrontal cortices, as well as cingulum and corticostriatal pathways. FA within this region was weakly associated with circulating levels of the inflammatory cytokine IL-6, but IL-6 did not mediate the social network and FA relationship. Finally, variation in FA indirectly mediated the relationship between social network diversity and intrinsic functional connectivity of medial corticostriatal pathways. These findings suggest that social integration relates to myelin integrity in humans, which may help explain the diverse aspects of health affected by social networks.

Aspects of the social environment affect physical health in humans. For example, increasing social integration predicts greater longevity and many positive long-term health outcomes (House et al. 1988; Berkman et al. 2000; Cohen 2004; Holt-Lunstad et al. 2010). Emerging research also shows that social network characteristics are associated with measures of neural integrity (Yang et al. 2013). For example, neuroimaging studies demonstrate that people with larger and more diverse social networks have larger brain volumes and greater functional connectivity in emotional salience processing networks (Bickart et al. 2011; Bickart et al. 2012), while larger social networks are indirectly associated with greater volume in the orbital prefrontal cortex, an area implicated in social cognition (Powell et al. 2012).

The relationship between social networks and the brain is not restricted to humans. In monkeys, neocortical regions important for processing social signals, including the rostral prefrontal cortex and amygdala, increase in volume with social network size (Sallet et al. 2011). Social isolation in adult mice causes reversible changes in prefrontal oligodendrocytes and hinders myelin repair in white matter (Liu et al. 2012). In young mice, however, the detrimental effects of social isolation on prefrontal myelin thickness are irreversible (Makinodan et al. 2012). The white matter changes in socially isolated animals associate with elevated pro-inflammatory cytokines like interleukin-6 (IL-6; (Hermes et al. 2006; Karelina et al. 2009)), suggesting a molecular basis for changes in the body with inflammation in the brain (Rosano et al. 2012). With the exception of a recent study examining overall brain volume (James et al. 2012), the human imaging literature has largely ignored the relationship between white matter integrity and social network structure. Yet a growing body of literature supports a

connection between inflammatory markers and aspects of an individual's social network. For example elevated IL-6 and C-reactive protein (CRP) levels are present in less socially integrated men (Häfner et al. 2011).

Furthermore, inflammatory cytokines are known to have a role in initiating "sickness behavior", which includes symptoms such as social withdrawal (Dantzer et al. 1998). It is possible that inflammation leads to feelings of social disconnection and withdrawal (Eisenberger et al. 2011). There is also emerging work showing a link between inflammation and white matter structure in humans (Arfanakis et al. 2013; Miralbell et al. 2012; Verstynen et al. 2013) and this pathway mediates relationships between social factors, like socioeconomic status, and white matter integrity (Gianaros et al. 2013). Taken together, these findings support the idea that aspects of the social environment relate to white matter structure in humans, possibly via inflammatory pathways.

Here we explored whether social network characteristics are associated with inflammation and white matter structure in humans. In a sample of neurologically healthy midlife adults we measured global white matter integrity using diffusion tensor imaging and evaluated social network size (number of people in the social network) and diversity (number of social roles) using the Social Network Index (Cohen et al. 1997). We hypothesized that more diverse and larger social networks would be associated with greater white matter integrity, i.e., larger fractional anisotropy and smaller radial diffusivity, and that this relationship would be mediated by circulating CRP and IL-6. We further predicted that these social associations with white matter have corresponding

implications for the functional dynamics of communication between connected brain areas.

Methods

Participants

Participants were 155 community-dwelling adults (78 men) who were recruited via mass mailings to residents of Allegheny County, Pennsylvania (U.S.A.). Table 1 lists all relevant participant demographics. A complete description of this sample is reported by Gianaros et al. 2013. All participants were screened for pre-existing health conditions. Informed consent was obtained prior to testing with approval from the University of Pittsburgh Institutional Review Board.

Social network assessment

All participants completed a questionnaire assessing the structure of their social networks. We evaluated two descriptive metrics of social networks that have been associated with neuromorphology or brain function (Bickart et al. 2011; Bickart et al. 2012).

(i) Diversity: assesses participation in 12 social roles (e.g., friends, family, church member). One point is assigned for each role (possible score of 12) for which respondents indicate that they speak (in person or on the phone) to someone in that relationship at least once every 2 weeks (Cohen et al. 1997).

(ii) Size: assesses the number of people with whom the respondent has regular contact (i.e., at least once every 2 weeks). To calculate network size, we computed the number of people with whom the respondent has regular contact

within each of the 12 social roles and then summed across the 12 roles (Cohen et al. 1997).

Physiological, psychosocial and health measures

We examined two markers of inflammation in a subset of subjects (N = 135 for CRP; N = 126 for IL-6).

(i) Interleukin-6 (IL-6) levels in pg/mL were determined using a high sensitivity quantitative sandwich enzyme immunoassay kit (R & D Systems). IL-6 levels were extrapolated from a standard curve with linear regression from a log-linear curve. All samples were run in duplicate, and the average coefficient of variation (CV) between samples was 10%. Prior to analysis, IL-6 values (mean = 1.79, std = 1.84) were natural log transformed.

(ii) Circulating levels of high-sensitivity C-reactive protein (CRP) in mg/dL were assayed on a SYNCHRON LX System (Beckman Coulter, Inc., Brea, California, with precision values of 5.0%CV within-run and 7.5%CV total for serum assays). Prior to analyses, CRP values (mean = 0.28, std = 0.47) were natural log transformed.

Two measures of socioeconomic status were also assessed at the initial testing session.

(i) Education was assessed by having participants report the number of years of schooling they had completed prior to the time of testing (mean = 17.12, std = 3.2).

(ii) Pre-tax income was assessed by having participants indicate their annual household earnings in U.S. dollars on a 15-point scale ranging from less than $10,000/year (or $0-833/month) to more than $185,000/year (or more than $15,417/month). See details on scale construction and computation in Gianaros et al. 2013.

Four measures of general physical health were collected.

(i) Waist circumference, as a measure of central adiposity, was measured at end-expiration to the nearest 1/2in with a tape measure centered at the umbilicus (mean = 35.64, std= 5.17 inches).

(ii) Seated, resting blood pressure was measured from the non-dominant arm with an oscillometric device (Critikon Dinamap 8100, Johnson & Johnson, Tampa, FL). Participants provided three measures taken 2 min apart after a ~20 min acclimation period, with the average of the last 2 of the 3 BP readings serving as the resting systolic (SBP) and diastolic (DBP) blood pressures (SBP, mean = 121.44, std = 9.48; DBP, mean = 73.25, std = 8.80).

(iii) Smoking status was measured by self-report, using a binary classification variable where 0 indicates non-smoker or former smoker, 1 indicates current smoker (25 smokers total).

(iv) Quality of sleep was measured using the Pittsburgh Sleep Quality Index (PSQI; Buysse et al. 1989) that ranks total sleep quality on a scale between 0 and 21, with scores 5 or less reflecting good sleep quality and scores greater than 5 reflecting poor sleep quality (mean = 4.53, std = 2.52).

Finally, we assessed trait positive and negative emotionality and social support.

(i) Dispositional positive and negative emotionality were assessed using the trait positive and negative affect scales of the Positive Affect (PA) and Negative Affect (NA) Schedule (Watson, Clark, & Tellegen, 1988; PA mean = 3.58, std = 0.59; NA mean = 1.61; std = 0.52).

(ii) Perceptions of social support were evaluated using the Interpersonal Support Evaluation List (ISEL) scale (Cohen et al. 1983). This is a list of 40 statements that focus on the perceived availability of potential social resources. (mean = 3.47, std = 0.45).

MRI Acquisition

All imaging was performed on a 3 Tesla Trio TIM whole-body MRI scanner (Siemens, Erlangen, Germany), equipped with a 12-channel phased-array head coil. Diffusion tensor imaging (DTI) was performed using a pair of pulsed-gradient, spin-echo sequences with a single-shot echo-planar imaging (EPI) readout. A parallel imaging algorithm (generalized auto-calibrating partial-parallel acquisition; GRAPPA) was applied during diffusion imaging to reduce echo-planar distortion. DTI parameters were: time-to-repetition (TR) = 5800 ms; time-to-inversion (TI) = 2500 ms; time-to-echo (TE) = 91 ms; flip angle = 90°; pixel size = 2 × 2 mm; resolution = 128 × 128 (with field-of-view [FOV] = 256 × 256 mm); 43 slices of 3 mm thickness with no gap; and total imaging time = 6 min and 19 s. Diffusion-sensitizing gradient encoding was applied in 30 uniform angular directions with a diffusion weighting of b = 1000 s/mm^2. A reference image with no diffusion gradient (b = 0) was also acquired. The acquisition sequence was repeated twice to improve the DTI signal-to-noise ratio. Usable DTI data were available for 145 participants.

Resting state functional BOLD images were acquired with a gradient-echo EPI sequence (FOV = 205×205 mm; 64×64 matrix; TR = 2 sec; TE = 28 ms; flip angle = 90°) for 5 minutes and 6 seconds. During scanning, participants were asked to keep their eyes open while resting quietly. Thirty-nine slices (3mm thick, no gap) were obtained for each TR, yielding 150 images (the first 3 images were discarded, allowing for magnetic equilibration). A structural image used for functional image co-registration and normalization was collected using a T1-weighted 3D magnetization-prepared rapid gradient echo (MPRAGE) sequence (FOV = 256×208 mm; 256×208 matrix; TR = 2100 ms; TI = 1100 ms; TE = 3.29 ms; flip angle = 8°; 192 slices; 1mm thick, no gap). Usable resting state data were available for 110 participants.

DTI Analysis

All DTI data were processed using the FSL Diffusion Toolbox (v2.0), which used the following steps: correction for motion and eddy current distortions by affine registration to the reference image, removal of skull and non-brain tissue, and calculation of diffusion parameters by fitting the diffusion images to a diffusion tensor model. Within each voxel three estimates of water diffusion patterns were calculated: fractional anisotropy (FA), radial diffusivity (RD) and axial diffusivity (AD). FA is a common white matter measure derived from DTI, and it represents the 'shape' of the underlying water diffusion in each voxel. AD and RD reflect subcomponents of the FA measure that define the length and width of the estimated tensor respectively.

All FA images were normalized to the $1mm^3$ MNI152 stereotaxic space via the FSL FA template (FMRIB58_FA). This was done by combining two transformations: (1) a

nonlinear registration of each participant's FA image to the FMRIB59_FA template, and (2) an affine transformation of the template to MNI152 space. These non-linear and linear normalization parameters were then applied to the axial and radial diffusivity maps. Finally, all maps for each subject were spatially smoothed using a $2mm^3$ FWHM isotropic Gaussian kernel.

To quantify head motion in each DTI scan we used a similar procedure to Yendiki et al., 2013. We calculated the average volume-by-volume translation and rotation, and the percentage of slices with signal dropout. Slices with a score greater than 1 have suspect signal dropout. Signal dropout severity was calculated over all slices in the scan that were greater than 1.

Structural connectivity was assessed on a tractography template (the CMU-60 template) comprised of averaged diffusion information across 60 neurologically healthy controls (29 male, mean age = 26) that underwent a 257-direction diffusion spectrum imaging sequence. Details of this template can be found here http://www.psy.cmu.edu/~coaxlab/?page_id=423 and the general procedures are described in Yeh & Tseng 2011. Clusters that were identified from the DTI analysis as being statistically significant to either SNI factor, after adjustment for multiple comparisons (FDR < 0.05) and cluster size (k>40), were loaded into the CMU-60 template. A set of 20,000 streamlines was tracked through this region of interest (fiber threshold = 0.05, max turning angle = 75 degrees, step size = 1mm). This set of streamlines was then hand segmented into 4 subsets (corpus callosum, cingulum, corticostriatal, and hypothalamic projections) based on pairwise start and end locations.

rs-fMRI Analysis

Resting BOLD images were preprocessed using SPM8 (http://www.fil.ion.ucl.ac.uk/spm/software/spm8/). BOLD images were realigned to the first series image, co-registered to the MPRAGE, and normalized to ICBM/MNI space using the SPM template. Normalized images were smoothed with a 6 mm FWHM isotropic Gaussian kernel and re-sliced to 2 mm^3 voxels. The contiguous clusters of the tractography endpoints larger than 50 voxels were selected as regions of interest (ROIs) for connectivity analysis. The connectivity between each pair of ROIs was assessed by the cross-correlation of the mean BOLD time series in the regions. Before the assessment, the time series in each voxel was de-trended, de-spiked, mean-centered, and adjusted for the confounding covariance due to movement, physiological noise, and hemodynamic response using regression method. The parameters estimated from rigid body transformation were used as the movement regressors. The physiological noise was modeled by the component-based method (Behzadi et al. 2007) with 3 principle components of BOLD time series from a white matter mask and 2 principle components from a CSF mask. The masks were constructed using the SPM MNI templates of 90% and 75% probability maps for white matter and CSF, respectively; they were further eroded to avoid partial volume effect. The hemodynamic response was modeled by the SPM default hemodynamic response function and its derivative. After the adjustment, the BOLD signals were bandpass filtered for the frequencies between 0.08 and 0.15HZ and submitted to the connectivity analysis.

Results

Social Network Size and Diversity

We first examined the associations of network indices with various demographic, social, affective, and health factors (See Table 1). In general both diversity and network size

were associated with similar measures, including age, income, education, PA and ISEL scores. Only network size was associated with current smoking status. There was no difference between men and women in social network size ($t(154) = 0.029$, $p = 0.33$) or diversity ($t(154) = 0.963$, $p = 0.87$). Moreover, neither network measure was associated with measures of physical or cardiorespiratory health. In the analyses below we control for central adiposity, age, sex, and years of education because these factors are plausible confounds of white matter structure and inflammatory measures.

Inflammation and social network structure

After controlling for central adiposity, age, sex, and years of education, IL-6 was negatively associated with the diversity of a person's social network ($r(128) = -0.194$, $p = 0.027$), but uncorrelated with social network size ($r(128) = -0.088$, $p = 0.319$). We did not find a relationship between network diversity and CRP ($r(137) = 0.04$, $p = 0.638$). CRP was also not correlated with social network size ($r(137) = 0.125$, $p = 0.144$). Finally, as expected CRP and IL-6 were moderately correlated with each other ($r(120) = 0.415$, $p < 0.0001$).

White matter and social network structure

We found that across all white matter voxels there was a predominant positive association between fractional anisotropy (FA) and diversity of a person's social network (mean = 0.012 +/- 0.039 std; Fig. 1a-b), after controlling for age, sex, education and central adiposity, which have all be found to be independently associated with measures of white matter integrity (Westlye et al. 2010; Gianaros et al. 2013; Verstynen et al. 2013). This means that in a numerical majority of voxels, individuals with more high-contact roles had greater microstructural white matter integrity. In the uncorrected

statistical maps we found several independent clusters with strong positive associations to diversity (Fig. 1a), including near prefrontal boundaries of the dorsal medial prefrontal cortex, considered part of the “social brain” (Lewis et al. 2011; Powell et al. 2012).

While there was a global positive association between network diversity and FA across a majority of voxels (Fig. 1a-b), this effect was particularly strong in a cluster of voxels near the posterior section of the genu of the corpus callosum (Fig. 1c). This large cluster of voxels surpassed both multiple comparison correction (FDR < 0.05) and cluster size thresholding (k > 40). No such patterns were observed for social network size, thus no further exploratory analysis was done on this measure.

To ensure that head motion did not interfere with the associations between SNI and FA (Yendiki et al. 2013), we ran a linear regression between the two SNI variables and head motion parameters. We found no significant correlations between SNI and head motion (all r’s < -0.137, all p’s > 0.11); thus spurious differences in head movement during the scans cannot account for the relationship between SNI diversity and FA that we detected.

In order to assess whether the association between SNI diversity and FA in this cluster is driven by particularly low diversity individuals, as would be predicted by the social isolation findings in rodents (Liu et al. 2012), we segmented the sample into three groups: low social diversity (< 5 roles, n = 38), moderate diversity (between 5 & 7 roles, n = 65), and high diversity (8 or more roles, n = 42). The unadjusted FA values within the corpus callosum cluster were extracted and averaged across groups. After controlling for age, sex, education and central adiposity, FA increased consistently with each diversity group (Fig. 2a), with a significant difference between low and high diversity individuals

(t(79) = 2.79, p = 0.008) and marginal differences between low and medium diversity groups (t(106) = 1.48, p = 0.14) and medium and high diversity groups (t(102) = 1.46, p = 0.14). Thus, the FA associations within this cluster are not driven exclusively by low or high diversity individuals.

Within the SNI-related cluster radial diffusivity (RD) decreased as social network diversity increased, after age, sex, education and central adiposity were controlled for (Fig. 2b; R = -0.15, p = 0.021). As with FA, we observed a significant difference between low and high diversity subjects (t(79) = 2.04, p = 0.044), but no difference between low and medium diversity individuals (t(106) = 1.55, p = 0.12) or medium and high diversity individuals (t(102) = 0.72, p = 0.47). Unlike RD, we did not observe a significant group effect on axial diffusivity within the cluster (Fig. 2c; R = - 6.55 x 10^{-7}, p = 0.45, Spearman's r(145) = -0.05, p = 0.200). This selective association with the radial component of the diffusion signal is consistent with patterns seen in animal models of demyelination (Klawiter et al. 2011).

Previous observations in rodents (Hermes et al. 2006; Karelina et al. 2009) predict that inflammatory factors should be moderately associated with white matter structure. Within the SNI-related cluster we found that, after controlling for age, sex, education and central adiposity, FA was negatively correlated with circulating levels of IL-6 (Fig. 3; Spearman's r(126) = -0.14, p = 0.017), and trending, but not significant, when correlated against circulating CRP (Spearman's r(135) = -0.12, p = 0.084). However, no such correlation was observed between IL-6 and either RD (r(126) = 0.07, p = 0.165) or AD (r(126) = -0.09, p = 0.096). This negative association between IL-6 and FA generally suggests that inflammation may be playing a role in white matter variation. However, this trend

disappears after controlling for age and sex (all p's > 0.1), thus negating IL-6 as a mediating variable within this sample.

Finally, we expanded our analysis to include a full set of psychosocial & health factors against the cluster-wise FA values. These results are shown in Table 2. Of these factors only smoking status correlated with FA within the target cluster. This association is consistent with a possible inflammation link to the FA variation in this region. However, given the lack of association with socioeconomic and general health factors that correlated with social network measures, it is unlikely that this SNI and white matter association is the mediated by socioeconomic (Gianaros et al. 2013) or physical health (Verstynen et al. 2013) pathways previously reported in this sample.

Network connectivity through SNI-related voxels

To characterize the pathways running through this cluster we performed deterministic tractography on a template of 60 neurologically healthy volunteers who were scanned using a high angular resolution form of diffusion imaging that is optimal for tractography in MNI space (see Methods). Using the SNI-related cluster as a region of interest, we found that a majority of the cluster covers interhemispheric connections between the superior and middle frontal gyrus (Fig. 4). The dorsal aspects of the cluster also include projections from the left cingulum tract while the ventral aspects intersect with portions of the superior infundibulum. Thus, the voxels having particularly strong associations with social network diversity predominantly reflect pathways connecting the left and right dorsolateral prefrontal cortex, with some carry over to fronto-parietal and limbic pathways.

To determine the extent that variation in the integrity of the white matter cluster associates with the functional properties of this connected circuit, we selected the cortical clusters of the tractography endpoints that had more than 50 contiguous voxels (ROIs; Fig. 5a) and used resting-state BOLD time series to evaluate the functional connections between all ROIs for each subject. After correcting for multiple comparisons (FDR < 0.05) and controlling for sex, age and central adiposity, one cluster pair was found to be negatively associated with FA within the SNI-related cluster (β = -1.09, p = 0.0146). This region reflected functional connections between an area on the superior frontal sulcus (SFG; center of mass (COM) in MNI-space = 22, 45, 30) and nucleus accumbens (NAcc; COM = 9, 7, 13), both in the right hemisphere. The diffusion component that explained the most variance between subjects' functional connectivity was the RD component (β = 652.30, p = 0.0016). Although the AD component was also associated with changes in functional connectivity (β = 351.95, p = 0.0286), this significance does not survive the threshold for multiple comparisons (Bonferroni adjusted p = 0.0167). Thus, within this corticostriatal pathway that runs through the SNI-associated cluster, we observed that individual differences in FA predict variance in functional connectivity, particularly with radial component of the DTI signal.

While white matter integrity correlated with functional connectivity of the corticostriatal pathway, social network diversity did not have a direct association with the functional connectivity between these regions (β = -0.0027, p = 0.36). However, because social network diversity is associated with white matter integrity within this cluster, it is possible that white matter serves as an indirect pathway linking SNI diversity with corticostriatal functional connectivity. Using a statistical mediation analysis (Preacher & Hayes 2008)

we found that FA (a*b = -0.0049, p = 0.0005) and RD (a*b = -0.0053, p = 0.0002) served as significant indirect pathways linking SNI diversity with corticostriatal functional connectivity (Fig. 5b). This indirect pathway was marginally significant with AD (a*b = -0.0013, p = 0.046) but this does not survive multiple comparison correction and the 95% confidence interval includes zero. Therefore, only FA and RD are indirect mediators linking social network diversity to corticostriatal functional connectivity.

Discussion

In a neurologically healthy group of midlife adults, we found that social network diversity correlated with the microstructural integrity of white matter pathways in the brain, particularly in an area near the anterior corpus callosum that includes multiple fiber pathways. This association was reflected as an increase in fractional anisotropy and decrease in radial diffusivity as social network diversity increases. In addition, white matter integrity in these voxels was associated with levels of inflammation. Both the pattern of anisotropy changes and association with inflammation are consistent with animal studies on the influence of the amount of social contact on myelin integrity (Liu et al. 2012; Hermes et al. 2006; Karelina et al. 2009). Any inferences between patterns in the diffusion signal and myelin or axonal changes are only speculative since the diffusion imaging signal is only an indirect measure of white matter microstructure and difficult to interpret in areas with crossing fibers (Wheeler-Kingshott and Cercignani 2009). Most importantly, we found that variation in SNI-related white matter indirectly mediates a relationship between social network diversity and functional connectivity of corticostriatal pathways, suggesting that the pattern of white matter variation may have an impact on functional processing as well (see also Bickart et al. 2012).

Recent neuroimaging work in humans has demonstrated the relationship between social network structure and general brain morphology (James et al. 2012; Bickart et al. 2012). Here we found decreased measures of white matter integrity (Liu et al. 2012; Makinodan et al. 2012) and increased inflammation (Hermes et al. 2006; Karelina et al. 2009) with decreased levels of social network diversity, results that are qualitatively consistent with evidence from studies of social isolation in mice. However, by assessing social network diversity as a continuous variable, our results suggest that it is not just the lack of social interaction that is associated with poorer brain health. Instead each increment in the diversity of one's network is associated with an increase in integrity. This may have important implications for understanding why greater diversity is associated with better cognitive function (Beland et al. 2005; Bennett et al. 2006; Ertel et al. 2008; Fratiglioni et al. 2000; Seeman et al. 2001; Tilvis et al. 2004; Zunzunegui et al. 2003).

Mechanistically, rodent models have shown that inflammation acts as a mediator between the amount of social isolation and reduced white matter integrity (Hermes et al. 2006; Karelina et al. 2009). Our results are also qualitatively consistent with this pathway in that reduced social network diversity correlated with reduced white matter integrity and increased systemic inflammation. While inflammation did not serve as an indirect mediator between white matter and social network structure, previous reports have found a direct link between white matter integrity and systemic inflammation throughout the human brain (Verstynen et al. 2013; Arfanakis et al. 2013; Wersching et al. 2010; Miralbell et al. 2012; Brück 2005). Inflammatory pathways reflect a general mechanism through which peripheral systems can interact with the central nervous system by visceral afferent transmission or by crossing the blood brain barrier (Banks et al. 1991; Ek et al. 2011; Hampel et al. 2005; Tracy 2002; Trapero & Cauli 2014; Yirmiya & Goshen 2011). Pro-inflammatory cytokines such as IL-6 are produced by microglia as

part of a normal brain cell functioning (Nakanishi et al. 2007; Shigemoto-Mogami et al. 2001). If the normal inflammatory immune response becomes chronic, increased levels of cytokines in the local microenvironment can lead to neuronal and glial dysfunction and death (Ramesh et al. 2013). Oligodendrocytes in particular may be more sensitive to raised levels of pro-inflammatory cytokines (di Penta et al. 2013). Furthermore, inflammatory cytokines are known to have a role in initiating "sickness behavior", which includes social withdrawal as a symptom (Eisenberger et al. 2011), and acute social stress leads to increased levels of IL-6 and TNF-α (Slavich et al. 2010). Inflammation could therefore have potential social psychological consequences, possibly playing a role in social withdrawal. With larger sample sizes, it may be possible to detect such relationships. Also, it should be noted that the white matter structural changes that occur as a result of inflammation in socially isolated rodents are observed under a more extreme measure of social integration than is used in humans. The stricter isolation that the rodents experience may have more observable consequences than measuring social diversity and number of contacts in a normal human population. Low power is likely a significant reason why we did not detect the same inflammation-mediated relationship between social network measurements and white matter integrity.

Previous human studies have also demonstrated a provisional association between measures of social network structure and both neuromorphology and brain function. In particular, Bickart and colleagues found that in humans, as social network size increases the volume of the amygdala is larger (Bickart et al. 2011) and the intrinsic functional dynamics increase between the amygdala and cortical areas related to social processing (Bickart et al. 2012). We found no correlation between social network size and pathways that directly innervate the amygdala itself. Instead, the portion near the

corpus callosum most strongly associated with social network diversity appears to interconnect the prefrontal, medial parietal and limbic areas. Functionally, this cluster is associated with changes in functional connectivity of corticostriatal pathways. However, the current findings are not necessarily mutually exclusive from the findings of Bickart and colleagues as the prefrontal cortex, striatum and amygdala are all known to have strong functional associations (Dolcos & McCarthy 2006; Kim et al. 2012; Lee & D'Esposito 2012; Golkar et al. 2012; Ochsner & Gross 2005). Therefore the gray matter and functional network differences in amygdala processing may not be detectible in the white matter pathways that innervate the nucleus. It is also possible that we did not have sufficient power in our sample to detect differences in the white matter pathways to the amygdala. More work is needed to bridge our white matter findings with the gray matter and functional network findings previously reported.

The fact that diversity-related variation in FA mediated corticostriatal functional connectivity implies that differences in social structure may have functional consequences for basal ganglia processing. Indeed, the dopaminergic pathways within cortico-basal ganglia loops have been indicated as being a key part of the so-called "social brain" (Skuse & Gallagher 2009). According to this model, inherent variation in sensitivity to feedback signals impacts an individual's likelihood to engage in social interactions. Unfortunately, given the cross-sectional nature of the current study, we cannot tell whether inherent differences in corticostriatal connectivity predisposes an individual to a particular social network structure or whether exposure to many high contact social roles modulates corticostriatal connectivity itself. Inferring the causal direction of these associations is left to future intervention or longitudinal studies.

Nonetheless, the current findings suggest that, like in rodents, reduced social network structure in humans is linked to the health of myelin in the brain. Our findings from the DTI analysis are largely consistent with variation in myelin integrity, and the simple correlation between FA and inflammation hints that similar molecular mechanisms may be mediating this effect in humans as in non-human animals. While previous work has linked both socioeconomic status (Gianaros et al. 2013) and physical health (Verstynen et al. 2013) to white matter integrity via inflammatory pathways, we believe that the social network associations reported here reflect an independent social-white matter link. This is supported by the fact that the voxels with the strongest network diversity and FA associations do not correlate with measures of socioeconomic status or general physical health (Table 2). Considering our current results in the context of previous findings suggests that different social factors can relate to brain morphology in different ways, but possibly through shared molecular pathways (e.g., inflammation). Thus, complex features of the broader social environment previously implicated in physical health (House et al. 1988; Holt-Lunstad et al. 2010; Uchino 2006; Cohen 2004) may also relate to the health of the brain. The extent to which these associations with neural integrity influence behavior should be a focus of future work.

References Cited

Arfanakis, K., Fleischman, D. , Grisot, G., Barth, C. M., Varentsova, A., Morris, M. C., … & Bennett, D. (2013). Systemic inflammation in non-demented elderly human subjects: brain microstructure and cognition. *PloS One*, *8*(8), e73107.

Banks, W. A., & Kastin, A. J. (1991). Blood to brain transport of interleukin links the immune and central nervous systems*. Life Sci*, 48, PL117-PL121.

Behzadi, Y., Restom, K., Liau, J., & Liu, T. T. (2007). A component based noise correction method (CompCor) for BOLD and perfusion based fMRI. *NeuroImage*, *37*(1), 90–101.

Beland, F., Zunzunegui, M. V., Alvarado, B., Otero, A., & Del Ser, T. (2005). Trajectories of cognitive decline and social relations. *J Gerontol B Psychol Sci Soc Sci*, 60, P320-P30.

Bennett, D. A., Schneider, J. A., Tang, Y., Arnold, S. E., & Wilson, R. S. (2006). The effect of social networks on the relation between Alzheimer's disease pathology and level of cognitive function in old people: a longitudinal cohort study. *Lancet Neurol*, 5, 406-12.

Berkman, L. F. (2004). Social Integration and Mortality: A Prospective Study of French Employees of Electricity of France-Gas of France: The GAZEL Cohort. *American Journal of Epidemiology*, *159*(2), 167–174.

Berkman, L. F., Glass, T., Brissette, I., & Seeman, T. E. (2000). From social integration to health: Durkheim in the new millennium. *Social Science & Medicine*, *51*(6), 843–57. Retrieved from

Bickart, K. C., Hollenbeck, M. C., Barrett, L. F., & Dickerson, B. C. (2012). Intrinsic amygdala-cortical functional connectivity predicts social network size in humans. *The Journal of Neuroscience*, *32*(42), 14729–41.

Bickart, K. C., Wright, C. I., Dautoff, R. J., Dickerson, B. C., & Barrett, L. F. (2011). Amygdala volume and social network size in humans. *Nature Neuroscience*, *14*(2), 163–4.

Brück, W. (2005). The pathology of multiple sclerosis is the result of focal inflammatory demyelination with axonal damage. *Journal of Neurology*, *252*, v3–9.

Buysse, D. J., Reynolds, C. F. III, Monk, T. H., Berman, S. R., & Kupfer, D. J. (1989). The Pittsburgh sleep quality index: A new instrument for psychiatric practice and research. *Psychiatry Research,* 28(2), 193-213.

Cohen, S. (2004). Social Relationships and Health. *American Psychologist*, *59*(8), 676–684.

Cohen, S., Doyle, W. J., Skoner, D. P., Rabin, B. S., & Gwaltney, J. M. (1997). Social ties and Susceptibility to the Common Cold. *Journal of the American Medical Association*, *277*, 1940–1944.

Cohen, S., & Hoberman, H.M. (1983). Positive events and social supports as buffers of life change stress. *Journal of Applied Social Psychology*, 13(2), 99-125.

Dantzer, R., Bluthe, R.-M., Gheusi, G., Cremona, S., Laye, S., Parnet, P., & Kelley, K. W. (1998). Molecular basis of sickness behavior. *Annals of the New York Academy of Sciences*, *856*, 132–138.

Di Penta, A., Moreno, B., Reix, S., Fernandez-Diez, B., Villanueva, M., Errea, O., … & Villoslada, P. (2013). Oxidative stress and proinflammatory cytokines contribute to demyelination and axonal damage in a cerebellar culture model of neuroinflammation. *PloS One*, *8*(2), e54722.

Dolcos, F., & McCarthy, G. (2006). Brain systems mediating cognitive interference by emotional distraction. *The Journal of Neuroscience*, *26*(7), 2072–9.

Eisenberger, N. I., Inagaki, T. K., Mashal, N. M., & Irwin, M. R. (2011). Inflammation and social experience: An inflammatory challenge induces feelings of social disconnection in addition to depressed mood. *Brain Behav Immun*, *24*(4), 558–563.

Ek, M., et al., (2001). Inflammatory response: pathway across the blood-brain barrier. *Nature,* 410(6827), 430-1.

Ertel, K. A., Glymour, M. M., & Berkman, L. F. (2008). Effects of social integration on preserving memory function in a nationally representative US elderly population. *Am J Public Health*, 98, 1215-20.

Fratiglioni, L., Wang, H. X., Ericsson, K., Maytan, M., & Winblad, B. (2000). Influence of social network on occurrence of dementia: a community-based longitudinal study. *Lancet*, 355, 1315-9.

Gianaros, P. J., Marsland, A. L., Sheu, L. K., Erickson, K. I., & Verstynen, T. D. (2013). Inflammatory pathways link socioeconomic inequalities to white matter architecture. *Cerebral Cortex*, *23*(9), 2058–2071.

Golkar, A., Lonsdorf, T. B., Olsson, A., Lindstrom, K. M., Berrebi, J., Fransson, P., … & Öhman, A. (2012). Distinct contributions of the dorsolateral

prefrontal and orbitofrontal cortex during emotion regulation. *PloS One*, *7*(11), e48107.

Häfner, S., Emeny, R. T., Lacruz, M. E., Baumert, J., Herder, C., Koenig, W., … & Ladwig, K. H. (2011). Association between social isolation and inflammatory markers in depressed and non-depressed individuals: results from the MONICA/KORA study. *Brain, Behavior, and Immunity*, *25*(8), 1701–7.

Hagmann, P., Jonasson, L., Maeder, P., Thiran, J., Wedeen, V. J., & Meuli, R. (2006). Understanding Diffusion MR Imaging Techniques: From Scalar Diffusion-weighted Imaging to Diffusion Tensor Imaging and Beyond. *RadioGraphics*, *26*, 205–223.

Hampel, H., et al., (2005). Pattern of interleukin-6 receptor complex immunoreactivity between cortical regions of rapid autopsy normal and Alzheimer's disease brain. *Eur Arch Psychiatry Clin Neurosci*, 255(4), 269-78.

Hermes, G. L., Rosenthal, L., Montag, A., & McClintock, M. K. (2006). Social isolation and the inflammatory response: sex differences in the enduring effects of a prior stressor. *American Journal of Physiology*, *290*(2), 273–82.

Holt-Lunstad, J., Smith, T. B., & Layton, J. B. (2010). Social relationships and mortality risk: a meta-analytic review. *PLoS Medicine*, *7*(7), e1000316.

House, J. S., Landis, K. R., & Umberson, D. (1988). Social Relationships and Health. *Science*, *241*, 540–545.

James, B. D., Glass, T., Caffo, B., Bobb, J. F., Davatzikos, C., Yousem, D., & Schwartz, B. S. (2012). Association of social engagement with brain volumes assessed by structural MRI. *Journal of Aging Research*, *2012*, 512714.

Jones, D. K., Knösche, T. R., & Turner, R. (2013). White matter integrity, fiber count, and other fallacies: the do’s and don'ts of diffusion MRI. *NeuroImage*, *73*, 239–54.

Karelina, K., Norman, G. J., Zhang, N., Morris, J. S., Peng, H., & DeVries, A. C. (2009). Social isolation alters neuroinflammatory response to stroke. *Proceedings of the National Academy of Sciences of the United States of America*, *106*(14), 5895–900.

Keller, B., Magnuson, T. M., Cernin, P. A., Stoner, J. A., & Potter, J. F. (2003). The significance of social network in a geriatric assessment population. *Aging and Clinical Experimental Research*, *15*(6), 512–517.

Kim, M. J., Loucks, R. A., Palmer, A. L., Brown, A. C., Kimberly, M., Marchante, A. N., & Whalen, P. J. (2012). The structural and functional connectivity of the amygdala: From normal emotion to pathological anxiety. *Behav Brain Res*, *223*(2), 403–410.

Klawiter, E. C., Schmidt, R. E., Trinkaus, K., Liang, H.-F., Budde, M. D., Naismith, R. T., … Benzinger, T. L. (2011). Radial diffusivity predicts demyelination in ex vivo multiple sclerosis spinal cords. *NeuroImage*, *55*(4), 1454–60.

Lee, T. G., & D'Esposito, M. (2012). The dynamic nature of top-down signals originating from prefrontal cortex: a combined fMRI-TMS study. *The Journal of Neuroscience*, *32*(44), 15458–66.

Lewis, P., Rezaie, R., Brown, R., Roberts, N., & Dunbar, R. I. M. (2011). Ventromedial prefrontal volume predicts understanding of others and social network size. *NeuroImage,* 57(4), 1624-1629.

Liu, J., Dietz, K., DeLoyht, J. M., Pedre, X., Kelkar, D., Kaur, J., … & Casaccia, P. (2012). Impaired adult myelination in the prefrontal cortex of socially isolated mice. *Nature Neuroscience*, *15*(12), 1621–3.

Makinodan, M., Rosen, K. M., Ito, S., & Corfas, G. (2012). A critical period for social experience-dependent oligodendrocyte maturation and myelination. *Science*, *337*(6100), 1357–60.

Miralbell, J., Soriano, J. J., Spulber, G., López-Cancio, E., Arenillas, J. F., Bargalló, N., … & Mataró, M. (2012). Structural brain changes and cognition in relation to markers of vascular dysfunction. *Neurobiology of Aging*, *33*(5), 1003.e9–1003.e17.

Ochsner, K. N., & Gross, J. J. (2005). The cognitive control of emotion. *Trends in Cognitive Sciences*, *9*(5), 242–9.

Powell, J., Lewis, P., Roberts, N., García-Fiñana, M., & Dunbar, R. I. M. (2012). Orbital prefrontal cortex volume predicts social network size: an imaging study of individual differences in humans. *Proceedings. Biological Sciences / The Royal Society*, *279*(1736), 2157–62.

Preacher, K., & Hayes, A. (2008). Asymptotic and resampling strategies for assessing and comparing indirect effects in multiple mediator models. *Behavior Research Methods*, *40*(3), 879–891.

Ramesh, G., MacLean, A. G., & Philipp, M. T. (2013). Cytokines and chemokines at the crossroads of neuroinflammation, neurodegeneration, and neuropathic pain. *Mediators of Inflammation*, *2013*, 480739.

Rosano, C., Marsland, A. L., & Gianaros, P. J. (2012). Maintaining brain health by monitoring inflammatory processes: a mechanism to promote successful aging. *Aging and Disease*, *3*(1), 16–33.

Sallet, J., Mars, R. B., Noonan, M. P., Andersson, J. L., O'Reilly, J. X., Jbabdi, S., … & Rushworth, M. F. S. (2011). Social network size affects neural circuits in macaques. *Science*, *334*(6056), 697–700.

Seeman, T. E., Lusignolo, T. M., Albert, M., & Berkman, L. (2001). Social relationships, social support, and patterns of cognitive aging in healthy, high-functioning older adults: MacArthur studies of successful aging. *Health Psychol*, 20, 243-55.

Skuse, D. H., & Gallagher, L. (2009). Dopaminergic-neuropeptide interactions in the social brain. *Trends in cognitive sciences*, *13*(1), 27-35.

Slavich, G. M., Way, B. M., Eisenberger, N. I., & Taylor, S. E. (2010). Neural sensitivity to social rejection is associated with inflammatory responses to social stress. *Proceedings of the National Academy of Sciences of the United States of America*, *107*(33), 14817–22.

Tilvis, R. S., Kahonen-Vare, M. H., Jolkkonen, J., Valvanne, J., Pitkala, K. H., & Strandberg, T. E. (2004). Predictors of cognitive decline and mortality of aged people over a 10-year period. *J Gerontol A Biol Sci Med Sci*, 59, 268-74.

Tracey, K. J. (2002). The inflammatory reflex. *Nature*, 420(6917), 853-9.

Trapero, I. & Cauli, O. (2014). Interleukin 6 and cognitive dysfunction. *Metab Brain Dis*., 29(3), 593-608.

Uchino, B. N. (2006). Social support and health: a review of physiological processes potentially underlying links to disease outcomes. *Journal of Behavioral Medicine*, *29*(4), 377–87.

Verstynen, T. D., Weinstein, A. M., Erickson, K. I., Sheu, L. K., Marsland, A. L., & Gianaros, P. J. (2013). Competing physiological pathways link individual differences in weight and abdominal adiposity to white matter microstructure. *NeuroImage*, *79*, 129–137.

Watson, D., Clark, L. A., & Tellegen, A. (1988). Development and Validation of Brief Measures of Positive and Negative Affect: The PANAS Scales. *Journal of Personality & Social Psychology*, 54(6), 1063-1070.

Wheeler-Kingshott, C. M., & Cercignani, M. (2009). About "axial" and "radial" diffusivities. *Magnetic Resonance in Medicine : Official Journal of the Society*

of Magnetic Resonance in Medicine / Society of Magnetic Resonance in Medicine, *61*(5), 1255–60.

Wersching, H., Duning, T., Lohmann, H., Mohammadi, S., Stehling, C., Fobker, M., … & Knecht, S. (2010). Serum C-reactive protein is linked to cerebral microstructural integrity and cognitive function. *Neurology*, *74*, 1022–1029.

Westlye, L. T., Walhovd, K. B., Dale, A. M., Bjørnerud, A., Due-Tønnessen, P., Engvig, A., ... & Fjell, A. M. (2009). Life-span changes of the human brain white matter: diffusion tensor imaging (DTI) and volumetry. *Cerebral cortex*, 20(3), 534-548.

Wu, Y.-H., & Bentler, R. A. (2012). Do older adults have social lifestyles that place fewer demands on hearing? *Journal of the American Academy of Audiology*, *23*(9), 697–711.

Yang, Y. C., McClintock, M. K., Kozloski, M., & Li, T. (2013). Social isolation and adult mortality: the role of chronic inflammation and sex differences. *Journal of Health and Social Behavior*, *54*(2), 183–203.

Yeh, F.-C., & Tseng, W.-Y. I. (2011). NTU-90: a high angular resolution brain atlas constructed by q-space diffeomorphic reconstruction. *NeuroImage*, *58*(1), 91–9.

Yeh, F.-C., Verstynen, T. D., Wang, Y., Fernández-Miranda, J. C., & Tseng, W.-Y. I. (2013). Deterministic Diffusion Fiber Tracking Improved by Quantitative Anisotropy. *PLoS ONE*, *8*(11), e80713.

Yendiki, A., Koldewyn, K., Kakunoori, S., Kanwisher, N., & Fischl, B. (2013). Spurious group differences due to head motion in a diffusion MRI study. *NeuroImage*.

Yirmiya, R. & Goshen, I. (2011). Immune modulation of learning, memory, neural plasticity and neurogenesis. *Brain Behav Immun*, 25(2), 181-213.

Yun, E. H., Kang, Y. H., Lim, M. K., Oh, J.-K., & Son, J. M. (2010). The role of social support and social networks in smoking behavior among middle and older aged people in rural areas of South Korea: a cross-sectional study. *BMC Public Health*, *10*.

Zunzunegui, M. V., Alvarado, B. E., Del Ser, T., Otero, A. (2003). Social networks, social integration, and social engagement determine cognitive decline in community-dwelling Spanish older adults. *J Gerontol B Psychol Sci Soc Sci*, 58, S93-S100.

Figure Captions

Figure 1. A) Uncorrected maps ($p < 0.025$) showing the voxels with strong positive (red) and negative (blue; none survive thresholding) associations with the social network index measure of diversity (SNI (Div)), and fractional anisotropy (FA). B) Probability distribution of regression coefficients between SNI (Div) and FA across all white matter voxels shown in panel A. The purple distribution shows the observed values while the gray distribution shows the average distribution shape across a set of randomized permutation tests designed to model the null effect. C) Location of the strongest cluster of voxels in the brain, with associations that survive multiple comparison corrections (FDR < 0.05) and clusterwise adjustments ($k>40$).

Figure 2. A) Average cluster FA for each SNI (Div) group. Subjects were assigned to groups based on which tertile of the social network distribution they fell into. The same values for axial diffusivity (AD) and radial diffusivity (RD) with the cluster are shown in panels B and C respectively. See text for statistical results. All errorbars show the standard error of the mean.

Figure 3. Scatterplot showing the negative correlation between clusterwise FA and IL-6 (natural log transformed).

Figure 4. Coronal, A, and sagittal, B, views showing the tracked fiber streamlines that run through the SNI (Div) related cluster (yellow region). Tractography was performed on the CMU-60 template brain.

Figure 5. A) Sagittal slices showing the eight regions of interest masks generated from cortical endpoints of tracked fiber pathways from analysis shown in Figure 4. These ROIs were used as masks for resting state functional connectivity analysis on the subset of the sample (N=110) that had viable resting state fMRI data. Variation in FA within the SNI (Div) related cluster correlated with variation in functional connectivity between a region on the right medial wall of the superior frontal gyrus and a region near the right nucleus accumbens (lower row). ACC, anterior cingulate cortex; PCC, posterior cingulate cortex; NAcc, nucleus accumbens; vmPFC, ventromedial prefrontal cortex; SFG, superior frontal gyrus; R, right; L, left. B) Mediation analysis showing how FA and RD served as indirect pathways linking SNI (Div) to functional connectivity of the significant corticostriatal pathway identified in A. Size of the lines represents the magnitude of the indirect (a^*b) pathway. Dashed lines indicate non-significant results after correcting for multiple comparisons. Bracketed numbers indicate the upper and lower bound of the bias corrected and accelerated 95% confidence interval for the indirect pathway.

	SNI Diversity		SNI #	
	r	p	r	p
Age	**0.173**	**0.031**	**0.159**	**0.048**
Sex	-0.004	0.960	-0.123	0.126
Income	**0.273**	**0.001**	**0.319**	**<0.0001**
Education (years)	**0.205**	**0.010**	**0.257**	**0.001**
Waist	0.018	0.820	0.015	0.856
SBP	0.040	0.623	0.104	0.197
DBP	-0.025	0.760	0.050	0.536
Smoking	β = -0.186	0.104	β = -0.062	0.210
PSQI (Duration)	-0.057	0.484	-0.087	0.290
PA	**0.214**	**0.008**	**0.241**	**0.003**
NA	-0.002	0.976	-0.077	0.340
ISEL	**0.187**	**0.020**	**0.170**	**0.035**

Table 1. Associations between demographic, socioeconomic, affective factors, and health factors and each social network measure. All associations except for smoking status were estimated using a non-parametric Spearman's rank order correlation test. Smoking status associations were determined using an iteratively reweighted binary regression routine. Statistically significant ($p < 0.05$ uncorrected) associations are indicated in bold.

	FA	
	r (N)	p
Age	-0.118 (145)	0.158
Sex	-0.047 (145)	0.578
Income	0.163 (141)	0.053
Education (years)	0.106 (145)	0.206
Waist	-0.133 (145)	0.112
SBP	-0.035 (145)	0.676
DBP	-0.063 (145)	0.450
Smoking	**β = 0.198 (145)**	**< 0.0001**
PSQI	-0.134 (142)	0.113
PA	0.048 (144)	0.569
NA	0.088 (144)	0.292
ISEL	0.087 (145)	0.299

Table 2. Associations between demographic, socioeconomic, personality factors, and health factors and FA within the target cluster. Same analysis and reporting conventions as used in Table 1.

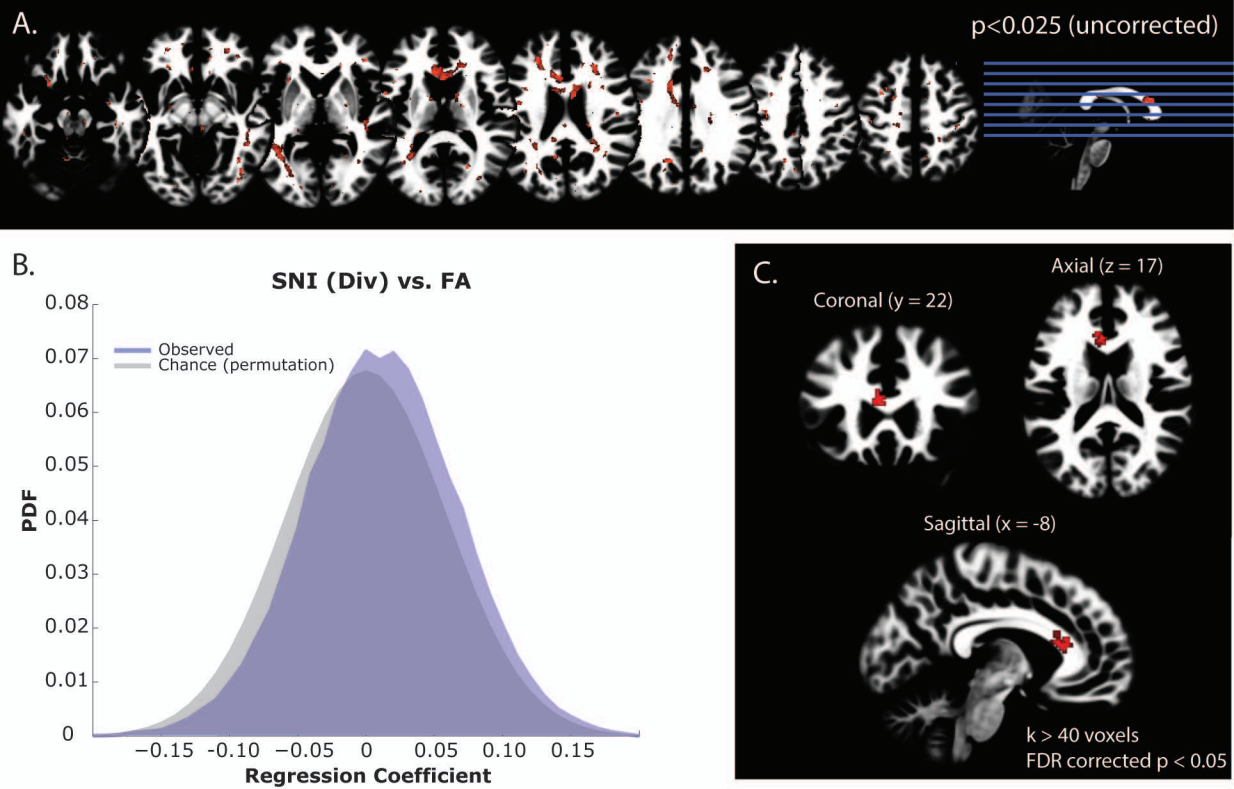
A.
p<0.025 (uncorrected)
B.
SNI (Div) vs. FA
Observed
Chance (permutation)
PDF
0.08
0.07
0.06
0.05
0.04
0.03
0.02
0.01
0
−0.15 -0.10 −0.05 0 0.05 0.10 0.15
Regression Coefficient
C.
Coronal (y = 22)
Axial (z = 17)
Sagittal (x = -8)
k > 40 voxels
FDR corrected p < 0.05

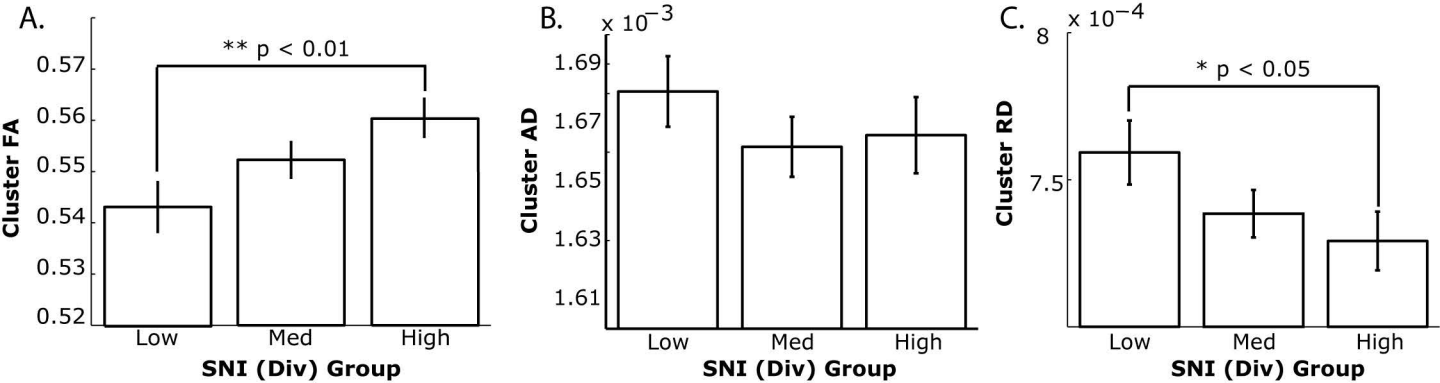
A.
** p < 0.01
Cluster FA
0.57
0.56
0.55
0.54
0.53
0.52
Low
Med
High
SNI (Div) Group
B.
x 10−3
Cluster AD
1.69
1.67
1.65
1.63
1.61
Low
Med
High
SNI (Div) Group
C.
x 10−4
8
* p < 0.05
Cluster RD
7.5
Low
Med
High
SNI (Div) Group

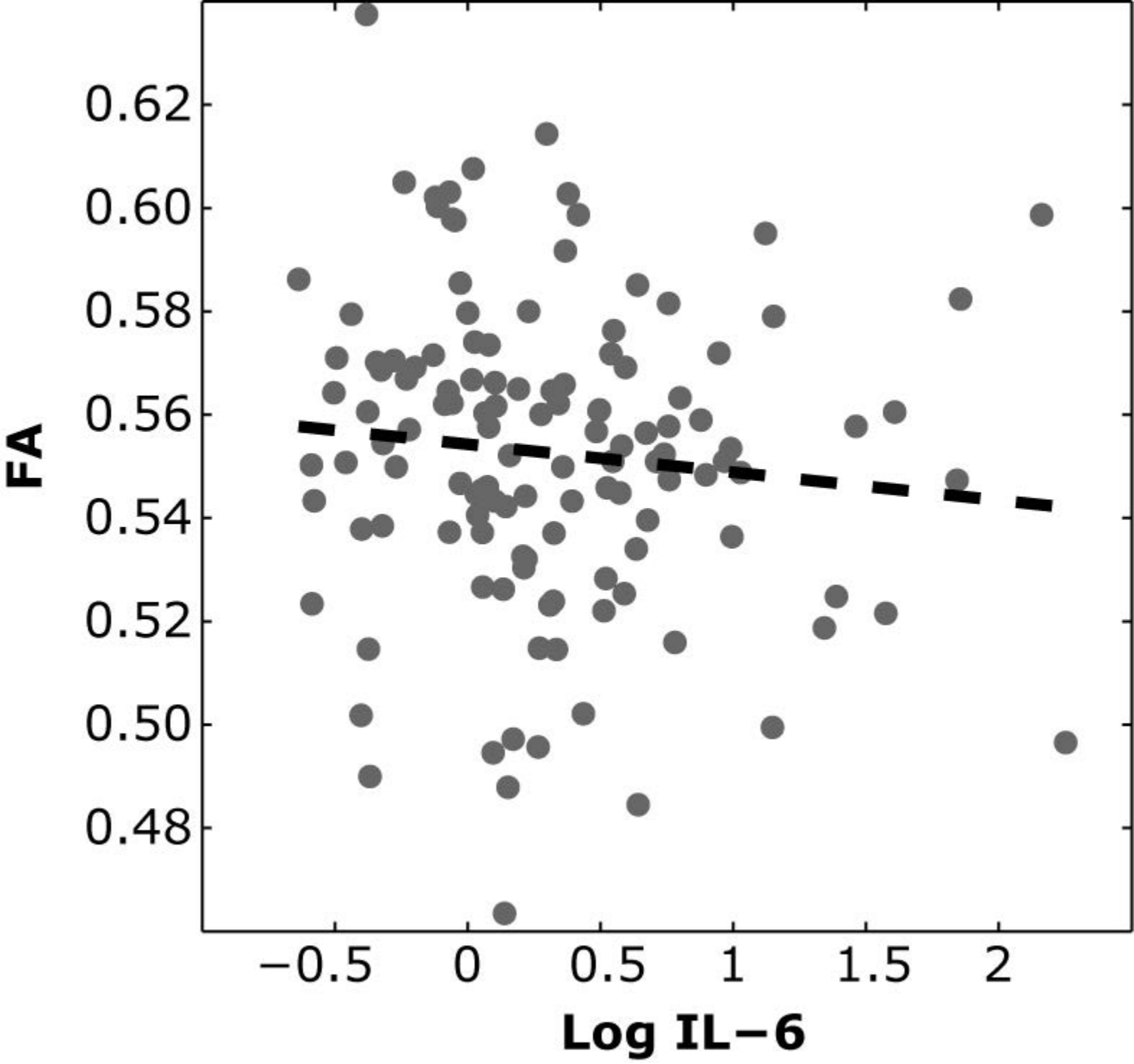
0.62
0.60
0.58
0.56
0.54
0.52
0.50
0.48
FA
−0.5
0
0.5
1
1.5
2
Log IL−6

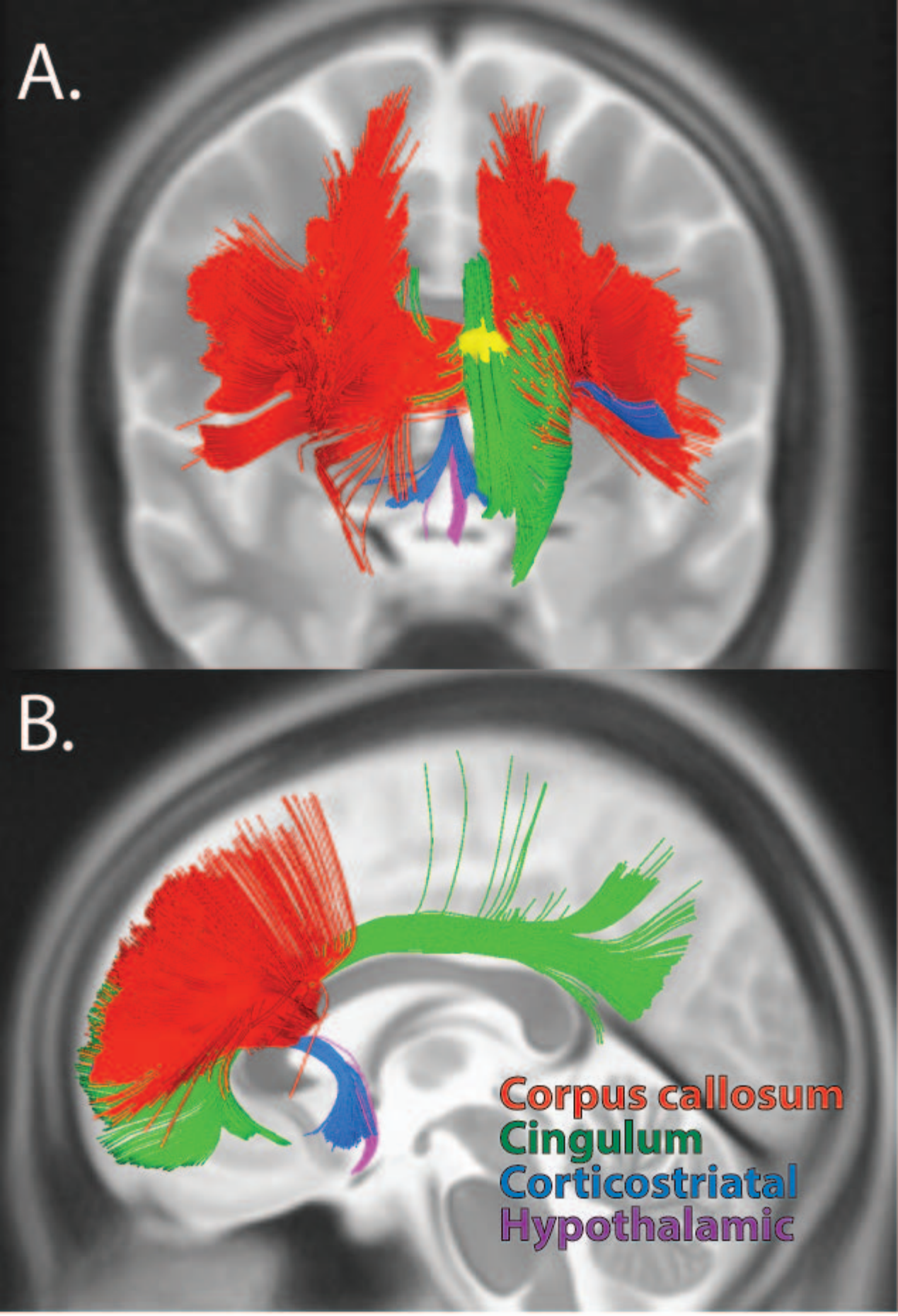
A.
B.
Corpus callosum
Cingulum
Corticostriatal
Hypothalamic

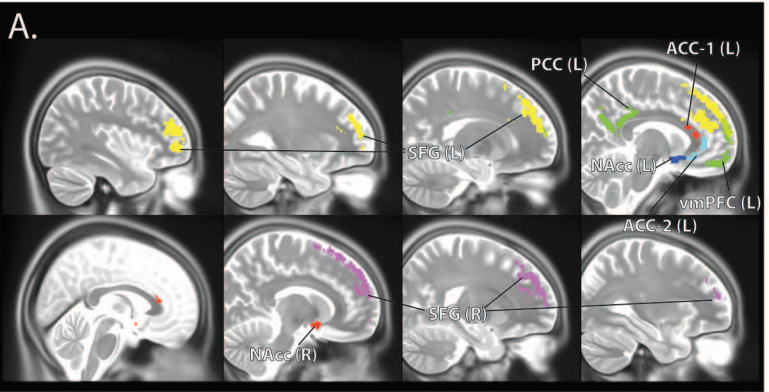
A.
PCC (L)
ACC-1 (L)
SFG (L)
NAcc (L)
vmPFC (L)
ACC-2 (L)
SFG (R)
NAcc (R)

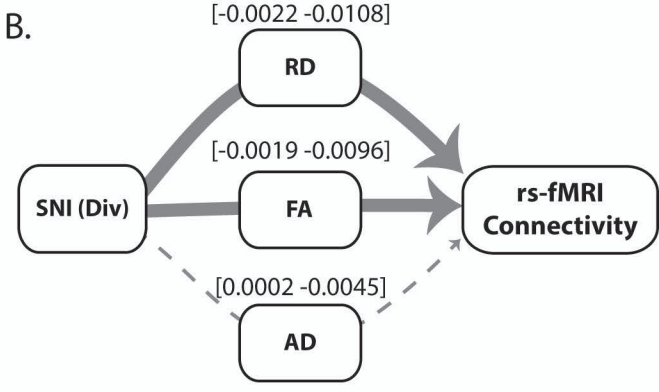
B.
[-0.0022 -0.0108]
RD
[-0.0019 -0.0096]
SNI (Div)
FA
rs-fMRI Connectivity
[0.0002 -0.0045]
AD